Earthquakes and Structures, *Vol. 18, No. 1* (*2020*) *129-145*
DOI: https://doi.org/10.12989/eas.2020.18.1.129

Seismic multi-level optimization of dissipative re-centering systems

Ivan Panzera*, Francesco Morelli[a] and Walter Salvatore[b]

Department of Civil and Industrial Engineering, University of Pisa, Largo Lucio Lazzarino 1, 56122 Pisa, Italy

(*Received July 26, 2019, Revised October 28, 2019, Accepted November 13, 2019*)

Abstract. Seismic resilience is a key feature for buildings that play a strategic role within the community. In this framework, not only the structural and non-structural elements damage but also the protracted structural dysfunction can contribute significantly to overall seismic damage and post-seismic crisis situations. Reduction of the residual and peak displacements and energy dissipation by replaceable elements are some effective aspects to pursue in order to enhance the resilience. Control systems able to adapt their response based on the nature of events, such as active or semi-active, can achieve the best results, but also require higher costs and their complexity jeopardizes their reliability; on the other hand, a passive control system is not able to adapt but its functioning is more reliable and characterized by lower costs. In this study it is proposed a strategy for the optimization of the dissipative capacity of a seismic resistant system obtained placing in parallel two different groups dissipative Re-Centering Devices, specifically designed to enhance the energy dissipation, one for the low and the other for the high intensity earthquakes. In this way the efficiency of the system in dissipating the seismic energy is kept less sensitive to the seismic intensity compared to the case of only one group of dissipative devices.

Keywords: seismic retrofit; passive control systems; optimization; energy dissipation; re-centering devices

1. Introduction

Strategic constructions with key roles in the economic and social life, as hospitals, civil protection buildings, industrial plants, infrastructures, etc., shall be characterized, in case of seismic events, by better performance than common buildings, in terms not only of higher safety levels for high intensity earthquakes but also of assuring the fully operability in case of low-to-moderate intensity earthquakes. Indeed, an eventual interruption of the activities foreseen in these structures can lead to unreasonable losses in economic and social terms. This awareness leaded in the last decades to the development of methods for the structural resilience assessment of strategic constructions (Cimellaro 2013, Hashemi *et al.* 2019) and networks (Cimellaro *et al.* 2013a, 2013b) and of tools and devices able to increase it, as, for example, dissipative devices. Such devices, indeed, are specifically designed to adsorb and dissipate the seismic energy entering in the construction, limiting the damage to the structural and non-structural elements and to the equipment focusing the damage to sacrificial elements, easy to repair or substitute at the end of the seismic event. Among all the families of dissipative and vibrations control devices, the most studied are generally the passive one (Christopoulos and Filiatrault 2006) characterized by a better reliability during earthquakes, lower costs and easier design process. In this context, numerous studies have been carried out in the last decades focusing on the influence of the device typologies adopted (Martinez-Rodrigo and Romero 2003, Dogruel and Dargush 2008) or of the mechanical characteristics of the single devices (Lee *et al.* 2018, Fateh *et al.* 2016, Hejazi *et al.* 2019) on the structural behavior, on the possibility of combining different devices (Lee *et al.* 2018, Belleri *et al.* 2017) or on the research of the disposition of the devices within the structure (Amouzegar *et al.* 2012, Wu *et al.* 1997, Ontiveros-pérez *et al.* 2003) that allows to optimize the global behavior.

The studies are, in all these cases, aimed at optimizing a structural performance parameter directly linked to the structural resilience, such as the reduction of the accelerations (Lin 2015) and damage (Hejazi *et al.* 2013, Belleri *et al.* 2017, Aguirre and Almazán 2015) and/or of the maximum (Ontiveros-pérez 2003, Laflamme 2018) or residual (Belleri *et al.* 2017, Lin 2015, Basu and Reddy 2016, Braconi *et al.* 2012, Morelli *et al.* 2016, Morelli *et al.* 2017a, Morelli *et al.* 2019) displacements, and the maximization of the dissipative capacity (Pekcan *et al.* 2014) or of the benefits/costs ratio (Hejazi *et al.* 2013, Belleri *et al.* 2017, Aguirre and Almazán 2015). Numerous other studies, instead, focused on multi-criteria or multi-performance optimization processes searching for a structural solutions that optimize a specific set of such aspects (Martinez-Rodrigo and Romero 2003, Pekcan *et al.* 2014, Vamvatsikos 2010, Greco and Marano 2016, Braga *et al.* 2019).

However, passive dissipative devices are, differently from semi-active and active systems, characterized by a pre-designed mechanical behavior that cannot be varied

*Corresponding author, M.Sc.
E-mail: ivanpanzera@gmail.com
[a]Ph.D.
E-mail: francesco.morelli@ing.unipi.it
[b]Professor
E-mail: walter@ing.unipi.it

http://www.techno-press.org/?journal=eas&subpage=7
ISSN: 2092-7614 (Print), 2092-7622 (Online)

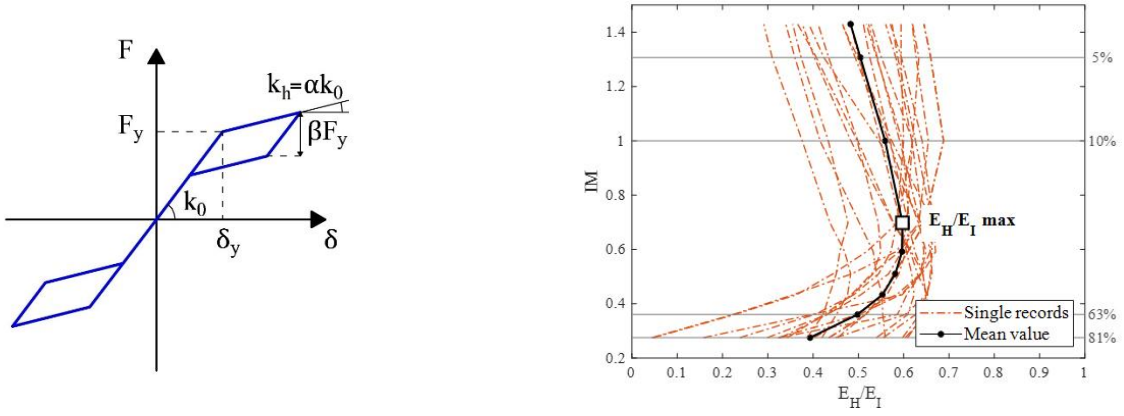

(a) (b)

Fig. 1 (a) Flag-shaped hysteretic curve typical of re-centering devices. (b) Variation, on the base of the seismic intensity, of the ratio between the energy dissipated by the re-centering devices, E_H, and the energy entered in the structure, E_I, in the study carried out by [1].

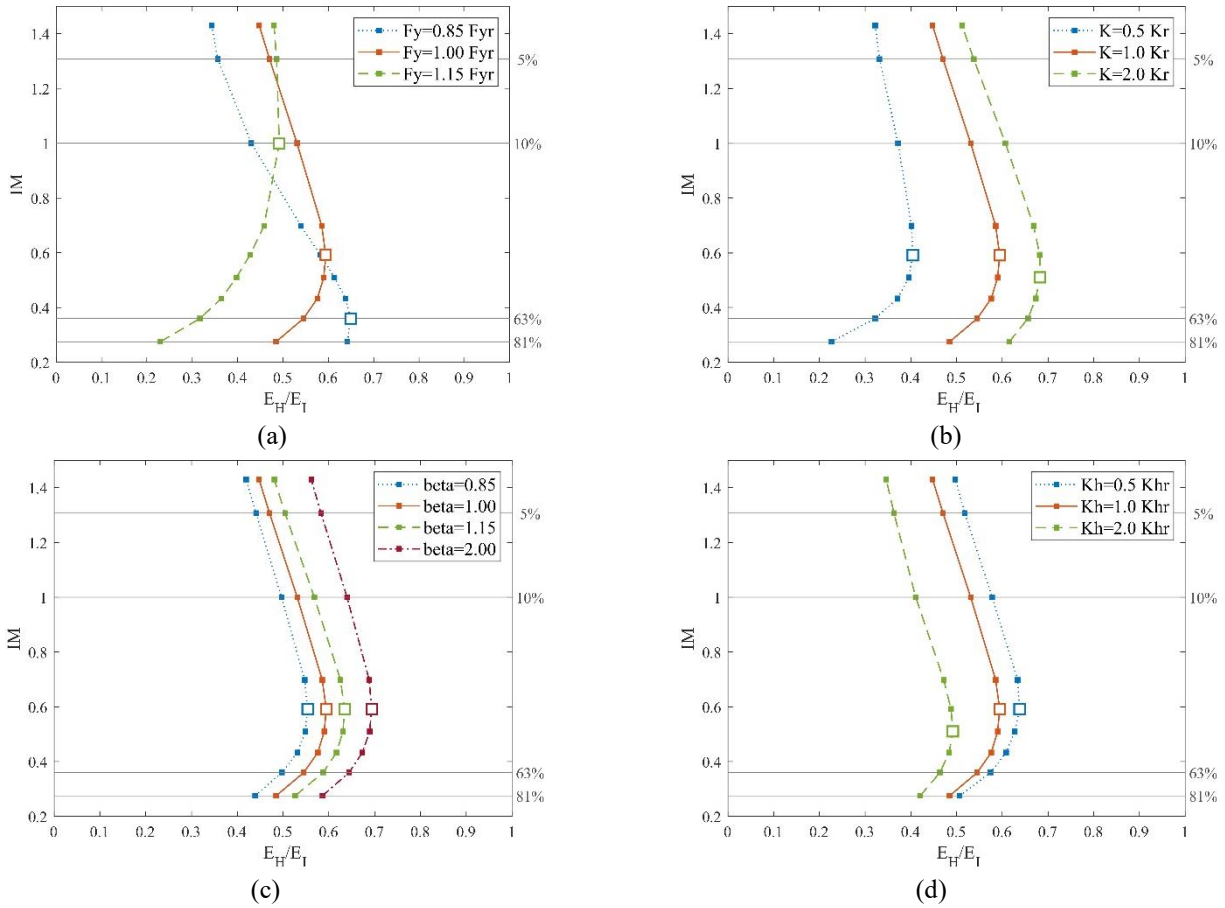

(a) (b)

(c) (d)

Fig. 2 Influence of the (a) opening force F_y, (b) initial stiffness k_0, (c) re-centering factor β and (d) post-opening stiffness k_h on the E_H/E_I ratio. The point corresponding to the maximum value of the E_H/E_I ratio isidentified by a square marker

depending on the seismic intensity, on the effective mass of the building in the instant the earthquake occurs or on the structural response. Therefore, they have the relevant disadvantage of being capable of optimizing the structural response or performance for a single level of the seismic action (Christopoulos and Filiatrault 2006). The research carried out in (Morelli *et al.* 2017a) highlighted this limitation in the case of the seismic retrofit of existing buildings through re-centering devices characterized by an hysteretic flag-shaped behavior, Fig. 1(a), showing that the ratio between the energy dissipated by the re-centering devices, E_H, and the energy entered in the structure, E_I, can be maximized only for a certain level of the seismic action, Fig. 1(b).

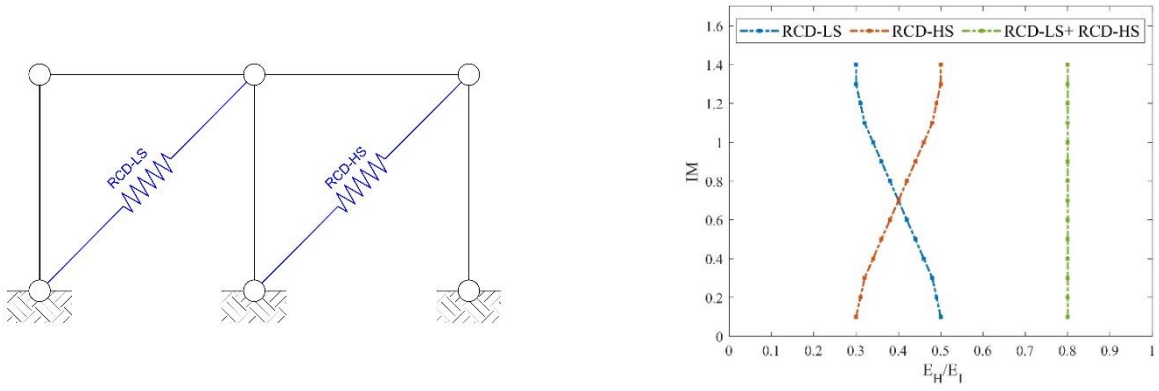

(a) (b)

Fig. 3 Schematic representation of the (a) re-centering dissipative devices working in parallel and (b) of the objective global E_H/E_I ratio vs. seismic intensity graph

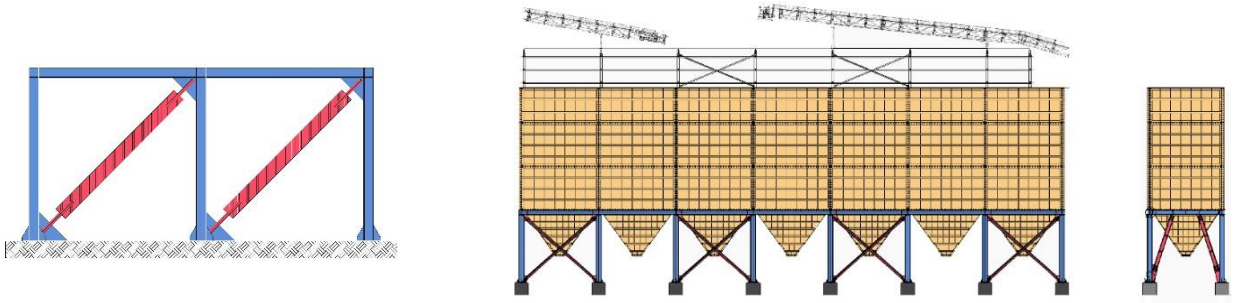

(a) (b)

Fig. 4 (a) General frame scheme used for the studying the optimization of the mechanical characteristics of the RCDs and (b) case study building adopted in the paper

The hysteretic behavior of the re-centering devices can be in general described by 4 parameters that completely define the flag-shaped hysteretic curve: the initial stiffness k_0, the opening force F_y, the post-opening stiffness $k_h=\alpha k_0$ and the re-centering factor β, as schematically shown in Fig. 1(a).

The study of (Morelli *et al.* 2017a) showed that the energy dissipation strongly depends, for a given structure, on each one of these parameters and each one of them influences in a different way the point for which the maximum E_H/E_I is obtained, see Fig. 2. In particular:

- The increasing of the opening force F_y, Fig. 2(a), allows to obtain the maximum E_H/E_I ratio for higher values of the earthquake intensity. The E_H/E_I ratio mean value evaluated over the earthquake intensity increases as F_y increases.
- The increasing of the initial stiffness k_0, Fig. 2(b), induces an increase of the E_H/E_I ratio mean value and reduces the earthquake intensity for which the peak dissipation is obtained.
- The increasing of the re-centering factor β, Fig. 2(c), increases the mean value of the E_H/E_I ratio and does not modify the intensity for which the peak dissipation is obtained.
- The increasing of the post-opening stiffness k_h, Fig. 2(d), induces a reduction of the E_H/E_I ratio mean value and decreases the intensity for which the peak dissipation is obtained.

In addition, Fig. 2(a) shows that low values of the opening force F_y of re-centering devices are optimal for low intensity earthquakes, while their efficacy in dissipating the seismic energy entering in the structure is reduced in the case of medium-to-high intensity earthquakes. On the contrary, high values of F_y are suggested for high and medium intensities and are not so effective for low seismic events.

An optimized dissipative solution, able to maximize the energy dissipated by the dedicated devices, should be characterized by a high and as constant as possible maximum value of the E_H/E_I ratio, independent of the seismic intensity.

The present research proposes an optimized solution based on the coupling of two different groups of re-centering devices (RCDs), see Fig. 3(a), one specifically designed to be characterized by a high dissipation capacity for low seismic actions (RCD-LS) and one for high seismic actions (RCD-HS). The resulting global energy dissipation capacity is also optimized through the selection of the mechanical characteristics that maximize the global dissipation capacity. The two groups of devices, working in parallel, can lead to a dissipation capacity less dependent on the earthquake intensity, see Fig. 3(b). E_H/E_I(IM) curves typically has their minimum value for maximum IM value in the case of RCD -LS and for minimum IM value in the case of RCD-HS.

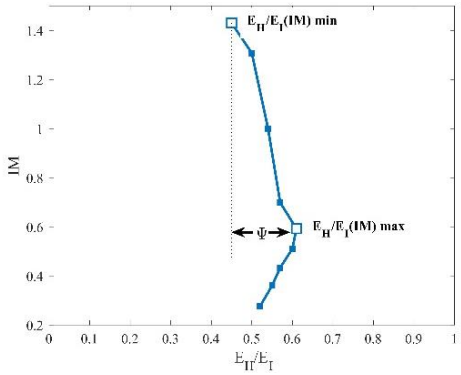

Fig. 5 Example of graphic representation of the two optimization parameters in terms of energy dissipation.

Table 1 Scenarios considered for the multi-objective optimization

	Weight of the goal "Maximization of $E_{DC,MAX}$"	Weight of the goal "Minimization of Ψ"
Scenario 1	1	0
Scenario 2	0.5	0.5
Scenario 3	0	1

This solution is applied to typical configurations of industrial buildings characterized by significant masses, such as supported silos. Such structural configuration is, indeed, particularly suited for the proposed solution considering that it can be schematized with a good approximation as a single degree of freedom system in each direction. Moreover, in these structures, very common in the industrial plants, the influence of superior modes can be neglected, allowing to highlight the pros and drawbacks of the proposed solution without including too many variables. To this end, the effects of including two types of re-centering devices working in parallel are first analyzed adopting the general scheme of Fig. 4(a), varying the parameters describing the hysteretic flag-shaped curve in order to find the set that maximize the dissipation capacity as a function of the mechanical behavior of the frames. Then, the optimization process is applied to a real case study, represented by the industrial building schematically represented in Fig. 4(b), aiming at the maximization of the dissipation capacity, taking into account, at the same time, also the structural checks and the standard codes provisions for the others structural elements.

2. Proposed optimization approach

The basic idea to increase the dissipation capacity of structures equipped with re-centering devices proposed within the present research is to include two distinct groups of devices with different hysteretic behavior, specifically designed to dissipate the seismic energy transmitted one by low-intensity earthquakes and the other by medium-to-high intensity earthquakes and the two groups of devices shall work in parallel.

The dissipation capacity of the structures equipped with the two groups of re-centering devices is strongly influenced by the hysteretic behavior of the devices themselves. For this reason and in order to be sure of analyzing an optimal solution, the hysteretic characteristics of the devices are selected through an optimization approach with two main goals:

•The maximization of the re-centering devices energy dissipation capacity, $E_{DC,MAX}$, numerically evaluated as

$$E_{DC,MAX} = \frac{E_H}{E_I}(IM)_{MAX} \quad (1)$$

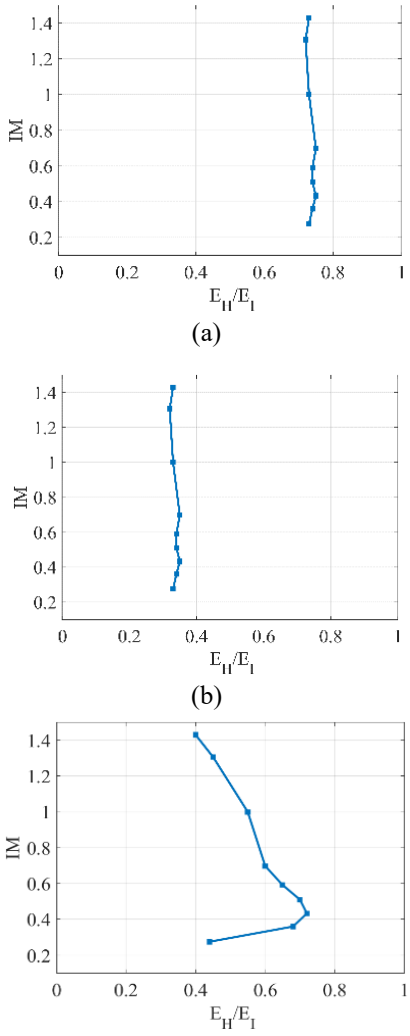

Fig. 6 Examples of possible energy dissipation capacities over the seismic intensity: (a) constant and high capacity,(b) constant but low capacity and (c) variable capacity over the seismic intensity

Table 2 Ranges of the mechanical parameters adopted for the optimization of the structural behaviour

RCD-LS		RCD-HS	
α_{LS}	0.1 - 0.3	α_{HS}	0.1 - 0.3
β_{LS}	0.9	β_{HS}	0.9
$r_{k,LS}$	4.3 - 5.7	$r_{k,HS}$	3.0 - 4.3
$r_{F,LS}$	0.4 - 0.9	$r_{F,HS}$	1.1 - 1.8

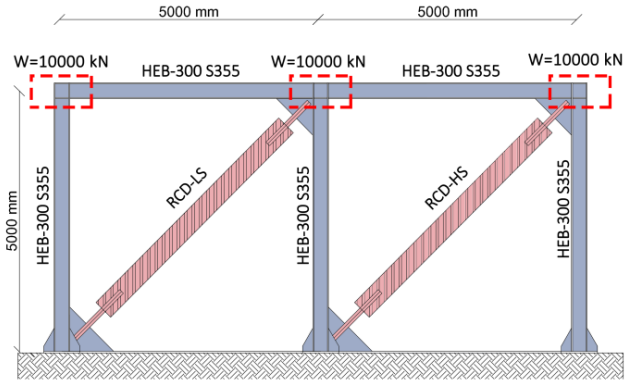

Fig. 7 Steel frame adopted for the optimization analyses

where, with reference to Fig. 5, IM is the Intensity Measure of the seismic action and E_H/E_I(IM) is the ratio of the energy entering the structure dissipated by the re-centering devices for a given IM.

• The minimization of the variability of E_H/E_I(IM) over IM, evaluated as the difference Ψ of the maximum, $E_H/E_I(\mathrm{IM})_{MAX}$, and the minimum, $E_H/E_I(\mathrm{IM})_{MIN}$, values

$$\Psi = \frac{E_H}{E_I}(IM)_{MAX} - \frac{E_H}{E_I}(IM)_{MIN} \tag{2}$$

From a theoretical point of view, the optimum configuration would be characterized by a high value of the energy dissipated by the devices E_H/E_I for every value of IM, Fig. 6(a). On the contrary, cases where E_H/E_I is low, Fig. 6b, or the dissipation is optimized only for limited values of the intensity level, Fig. 6(c), shall be avoided.

The optimization of the re-centering devices hysteretic behaviors, aimed at the maximization of $E_{DC,MAX}$ and the minimization of Ψ, is consequently a multi-objective optimization and can be carried out giving more importance to a single goal or to the other. In order to study the effects of the optimization on different situations, the three different scenarios, resumed in Table 1, were considered.

Scenario 1 and Scenario 3 represent respectively the cases in which only the maximization of $E_{DC,MAX}$ or only the minimization of Ψ are pursued, while Scenario 2 is the case in which both the objective have the same weight in the research of the optimal solution.

The optimization analyses were carried out considering the general steel frame of Fig. 7, where typical dimensions and masses of an industrial structure were considered.

2.1 Optimization procedure of the hysteretic parameters

The optimization is carried out varying the parameters describing the hysteretic behavior of each group of the re-centering devices. These parameters allow to completely define the flag-shaped hysteretic behavior and are: the initial stiffness k_0, the opening force F_y, the post-opening stiffness $k_h=\alpha k_0$ and the re-centering factor β, as schematically shown in Fig. 1(a).

To take into account also the contribution in terms of stiffness and resistance of the frame in which the re-centering devices are inserted, the initial stiffness k_0 and opening force F_y are normalized by the initial stiffness $k_{0,MRF}$ that the single bare frame offers to the horizontal actions applied at the beam level and by the corresponding yielding force $F_{y,MRF}$

$$r_k = \frac{k_0}{k_{0,MRF}} \tag{3}$$

$$r_F = \frac{F_y}{F_{y,MRF}} \tag{4}$$

A "blind" parametric analysis considering the whole ranges of variation of the 4 parameters and considering all the possible combinations would require enormous computational time that can be instead reduced following a more rational process. Within this research the range of variation of the four parameters was reduced on the base of simple and logical considerations about the global structural behavior desired and the RCD's hysteretic behavior:

• In order to allow the group of RCD-LS to dissipate the higher ratio of the energy transmitted by low-intensity earthquakes, its initial stiffness $r_{k,LS}$ shall be higher than the initial stiffness of the group in charge of dissipating the seismic energy transmitted by the high intensity earthquakes, RCD-HS.

• The group of RCD-LS shall be characterized by a value of $r_{F,LS}$ lower than 1, allowing the seismic energy dissipation in the RCDs also for low values of the earthquake intensity.

• The factor β represents a compromise between the re-centering force and the dissipation capacity of the re-centering device. Values of β close to 0 means the absence of dissipation capacity and the maximum re-centering force. On the contrary, values close to 2 represent hysteretic cycles without re-centering capacity. Within the present research, to assure a compromise between the re-centering and the dissipation capacities and to limit the parameters that need to be varied, β was assumed as a constant value equal to 0.9.

On the basis of such considerations, the range of variations of Table 2 were considered.

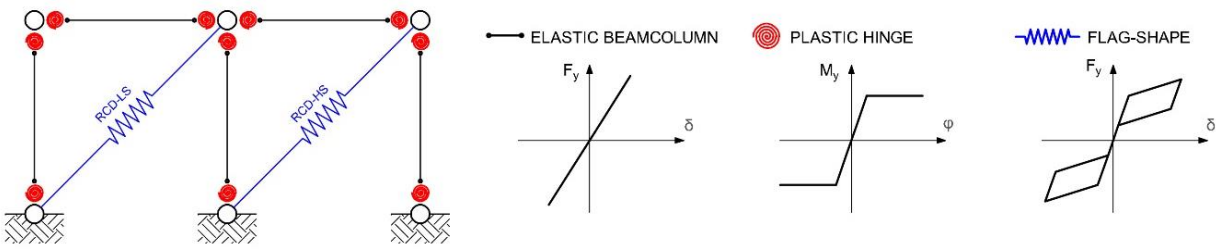

Fig. 8 Numerical model of the steel frame with the two groups of RCDs

Table 3 Ground motions used for the execution of the Incremental Dynamic Analyses

DB	ID	Earthquake Name	Mw	Fault. Mec.	R(kM)	Site Class	Date
ED	1257	Izmit	7,6	Strikeslip	20	C	17/08/1999
ED	196	Montenegro	6,9	Thrust	25	B	14/04/1979
ED	535	Erzincan	6,6	Strikeslip	13	B	13/03/1992
ED	6349	South Iceland	6,4	Strikeslip	5	A	21/06/2000
ED	74	Gazli	6,7	Thrust	11	D	17/05/1976
IN	113	South Iceland	6,5	Strikeslip	5,25	A	17/06/2000
IN	331	Darfield	7,1	Strikeslip	17,82	C	03/09/2010
IN	445	Imperial Valley	6,5	Strikeslip	27,03	C	15/10/1979
IN	451	Loma Prieta	6,9	Oblique	7,1	B	18/10/1989
IN	461	Northridge	6,7	Reverse	20,25	C	17/01/1994
IN	466	Duzce	7,1	Strikeslip	5,27	C	12/11/1999

	Vr	P_{vr}	λ	Tr	ag	S.F.
	yrs	%	1/yrs	yrs	g	\
0	100	4%	0.0004	**2475**	0.512	1.43
1	100	**5%**	0.0005	1950	0.4687	1.307
2	100	**10%**	0.0011	949	0.3586	**1.000**
3	100	22%	0.0025	402	0.2502	0.698
4	100	30%	0.0036	280	0.2122	0.592
5	100	39%	0.0049	202	0.1829	0.510
6	100	50%	0.0069	144	0.1552	0.433
7	100	**63%**	0.0099	101	0.1292	0.360
8	100	**81%**	0.0166	60	0.0987	0.275

(a)

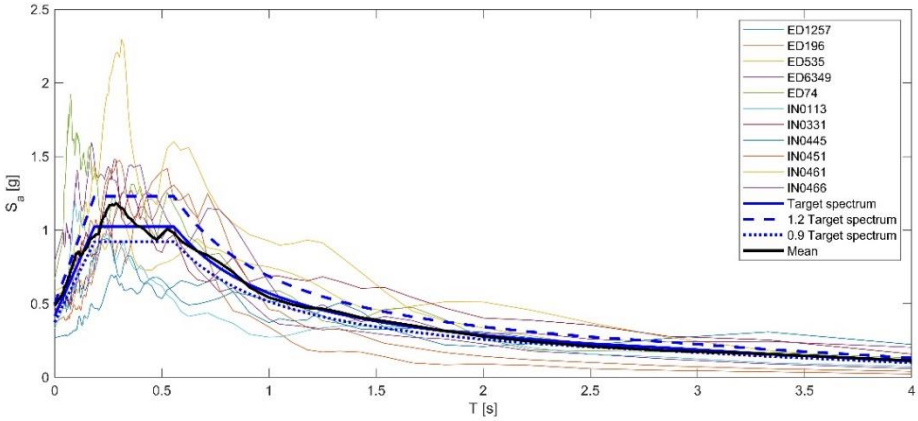

(b)

Fig. 9 (a) Scale factors, S.F. adopted (b) ground motions response spectrum

In order to find the set of these four parameters that, depending on the geometrical and mechanical characteristics of the structure to protect and on the seismic intensity, maximizes the re-centering device energy dissipation, a parametric incremental dynamic analysis on the single storey steel frame of Fig. 7 was carried out. The same analyses were carried out also considering the case in which the two groups of devices have the same characteristics highlighting the advantages and drawbacks of the proposed configuration of RCDs.

2.2 Modelling approach

The parametric incremental dynamic analyses were carried out through a non-linear model realized in OpenSEES (Mazzoni *et al.* 2006), modelling the beams and the columns of the steel frame through lumped plasticity elements, while the RCDs were modelled using truss elements with flag-shaped hysteretic behavior, see Fig. 8. To carry out the parametric Incremental Dynamic Analyses, a Uniform Hazard Spectrum-coherent method was adopted for the ground motions selection. The eleven ground motions recordings adopted in (Morelli *et al.* 2017a) were used, see Table 3, considering that they were selected following the indications of the main international standards, assuring the consistency with the seismic characteristics of the source. The reference spectrum was matched with the geometric mean (GeoMean) of the two horizontal ground motions components, ensuring that the mean spectral ordinates of each set are never lower 90% of the reference spectrum in the period range between 0 s and 2 s, consistent with the spectrum-matching requirements of Eurocode 8 (§3.2.3.1 EN 1998-1-2011). The complete procedure of the ground motion selection, together with all the background and motivations, is described in (Morelli *et al.* 2017b, Faggella *et al.* 2016).

2.3 Results of the optimization

Fig. 10 reports, for the three scenarios analyzed, the IDA curves of the energy dissipated E_H/E_I by the RCDs for both the case of two groups of devices with distinct characteristics (respectively RCD-LS and RCD-HS) and the case of devices with equal behavior. The mehcanical parameters of the optimized devices for the three scenarios considered and for the two configurations proposed (two groups of devices with equal or with different characteristics) are reported in Table 4.

The results illustrated in Fig. 10 highlight important aspects of the device configurations studied. If the objective of the optimization is the maximization of the $E_{DC,MAX}$ (scenario 1, see Fig. 10(a)), as defined in equation (1), the

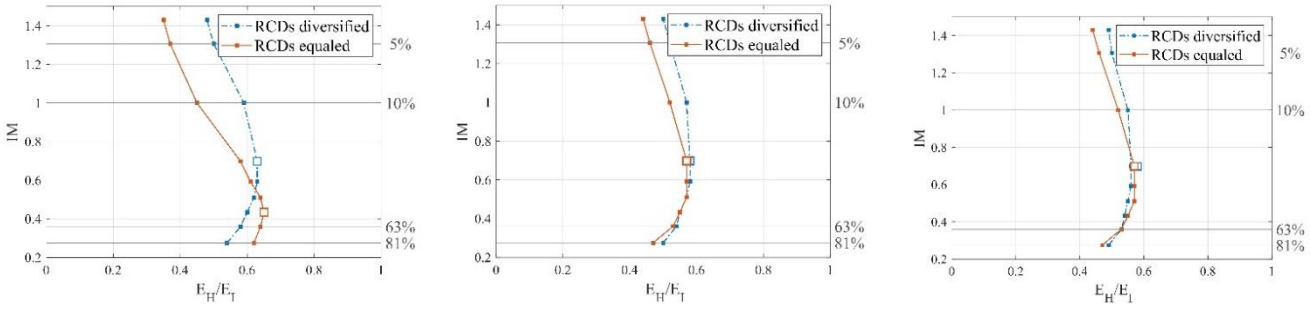

(a) (b) (c)

Fig. 10 IDA curves of the energy E_H/E_I dissipated by the RCDs for the scenarios (a) 1, (b) 2 and (c) 3

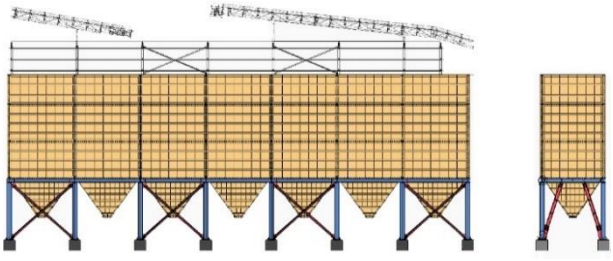

Fig. 11 Front views of the building in the longitudinal (left) and transversal (right) directions

Table 4 Mechanical parameters of RCDs obtained from the optimization procedure

	RCDs with equal behavior			RCDs diversified for Low and High seismic levels					
	α	r_k	r_F	α_{LS}	α_{HS}	$r_{k,\,LS}$	$r_{k,\,HS}$	$r_{F,\,LS}$	$r_{F,HS}$
Scenario 1	0.1	6.5	0.4	0.1	0.1	8.5	4.5	0.5	1.0
Scenario 2	0.1	6.5	0.4	0.2	0.1	8.5	4.5	0.4	1.4
Scenario 3	0.3	6.5	0.6	0.2	0.1	8.5	4.5	0.4	1.4

strategy of adopting two distinct groups of RCDs leads to better results than adoption of RCDs with equal characteristics also in terms of minimization of the variability Ψ of E_{CD}(IM) over IM, evaluated as in equation (2). If the objectives of the optimization are both the maximization of $E_{DC,\mathrm{MAX}}$ and the minimization of Ψ (scenario 2, see Fig. 10(b)), the results are still better for the case of adopting two groups of RCDs being its optimized dissipation capacity, E_{CD}(IM), always higher than the case of a single group of RCD with equal characteristics and the variability Ψ of E_{DC}(IM) over IM very similar in the two cases. Finally, when the objective of the optimization is the minimization of Ψ (scenario 2, see Fig. 10(c)), the strategy of adopting two different groups of RCDs does not show significant advantages respect to the case of using RCDs with equal behavior.

3. Structural modelling and analysis of the case study

In order to study the effect of the proposed optimization considering also the limitations induced by the necessity of executing the structural checks of the building elements in which the RCDs are included and the different operative conditions of the building itself, the optimization process was then applied to retrofit an existing industrial building.

The building is a group of seven silos supported in both directions by a concentrically and eccentrically braced structure belonging to a steel making plant, see Fig. 11; two different operational conditions were considered assuming the silos full up to the 50% and 75% of the total capacity in order to evaluate the efficiency variation of the design choices arising from the optimization procedure. The case with the silos completely full (100% of the total capacity) was not taken into account because in this situation the columns almost reach the buckling resistance and even a little horizontal seismic load induce the collapse of the structure. This situation is typical in industrial building optimized for the static loads and originally designed neglecting the influence of the seismic action. Moreover, the condition in which the silos are all completely full is very rare and the probability of having it when a strong earthquake occurs is practically negligible.

The silos are firmly connected each other and can be considered as a single rigid body. Considering that only plane analyses on the longitudinal direction were carried out, the whole structure can be assumed as a single degree of freedom system.

The case study was firstly analyzed through Incremental Dynamic Analysis in the as-it-is state in order to evaluate the seismic vulnerability and then retrofitted substituting the existing bracings with RCDs adopting the strategy of including the two groups of different devices, RCD-LS and

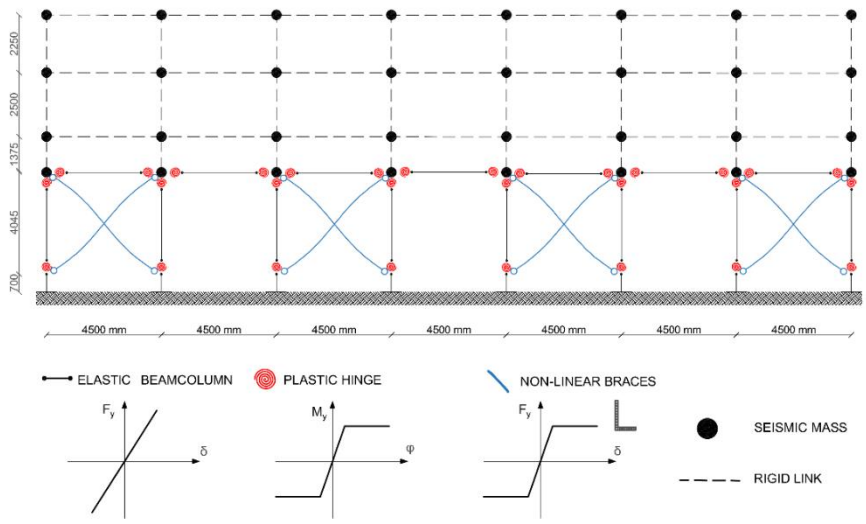

Fig. 12 Global view of the numerical model adopted

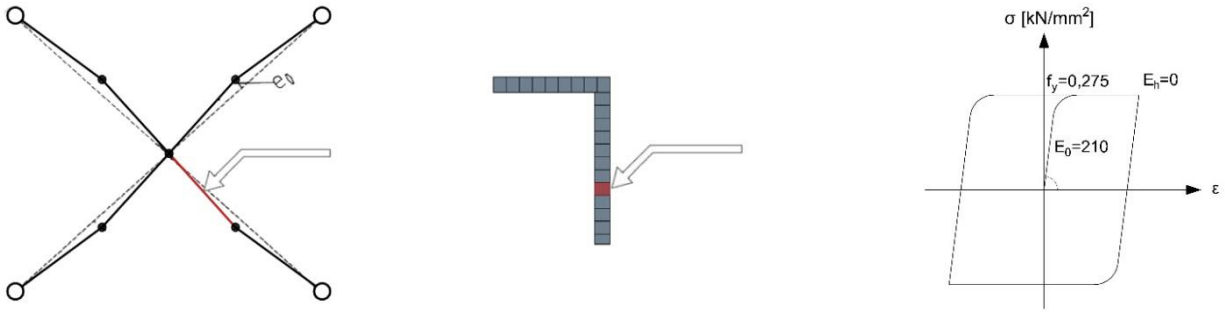

(a) (b) (c)

Fig. 13 Modelling of the bracings: (a) geometry and local bow imperfection, (b) fiber section and (c) steel stress-strain relationship

RCD-HS.

3.1 Modelling

The case study building was modelled considering the upper part, including all the silos, as a rigid body and analyzing therefore only the structural behavior of the support frames. The silos and the infill material were considered as dead load and seismic masses, while the bracings are pinned to the beam-to-column joints, see Fig. 12.

The bracings are made up of double *L* profiles (L130×90×12) with S275 steel grade and they are connected in the middle by a single bolt. Following the indications of the Italian guidelines (CNR-UNI 10011-1988), the bolt, having a shear resistance higher than 1/5 of the bolts placed at the end connections, can be considered capable of reducing the free buckling length of the bracings themselves. The bracings have been therefore modelled considering a local bow imperfection equal to 1/200 of their semi-length, see Fig. 13(a), adopting a corotational geometry transformation (Mazzoni *et al.* 2007) that allows to consider in each step the effective deformed shape and updating therefore the stiffness matrix to take into account the II order effects. For each bracing it was then checked that the resulting buckling load obtained through the numerical model was similar to the one obtained applying the provisions of Eurocode 3 (EN 1993-1-1-2011), see Fig. 14. The cross section was modelled adopting fiber elements, assigning to each fiber an elasto-plastic behavior.

The beams (HEB280A S275 sections) were modelled as simply nonlinear element with plastic hinges at both end, while the model of the columns (HEB280A S275 sections) takes into account also the II order effects through a P-Delta geometrical transformation (Mazzoni *et al.* 2007).

All the other elements of the buildings such as the silo's walls, the conveyor belts and the infill material were modelled as lumped masses. The location of the lumped masses was defined taking into account the two filling conditions of the silos (50% and 75%) considered in the analyses and concentrating the whole mass in the center of gravity of the corresponding volume of competence, with a total of 4 lumped masses for each silo distributed along the height, see Fig. 15.

3.2 Definition of limit states

The assessment of the seismic behavior of the case study building in its as-it-is state and in the retrofitted state, the latter presented in the following paragraphs, took into account the assessment of the limit states of the structural elements as defined by Eurocode 8 (EN 1998-3-2005). For

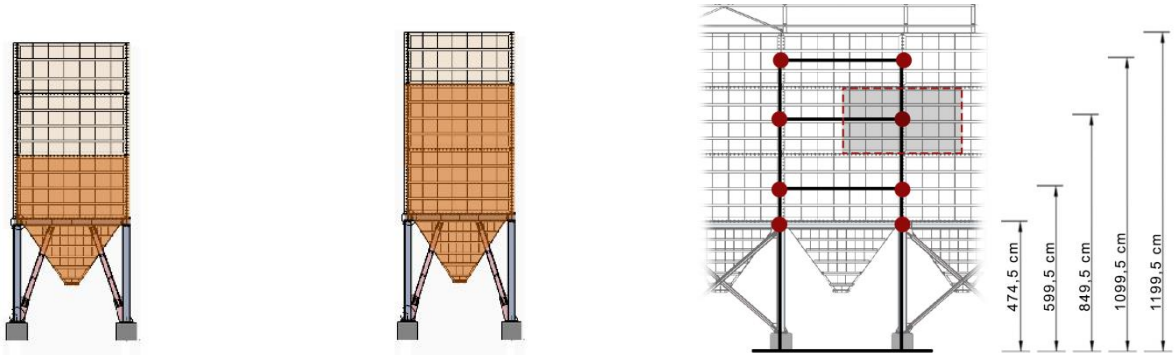

(a) (b) (c)

Fig. 15 Considered filling conditions of the silos: (a) 50%, (b) 75% and (c) location of the lumped masses in the numerical model

Table 5 Deformation associated to the Limit States considered in the analyses: Significant Damage (SD), Near Collapse (NC)

Element	Definition of the limit states				δ rigid floor [mm]	
	Type	Elastic Limit	SD	NC	SD	NC
Columns – HE280A	Rotation	$\Delta\gamma$=12mrad	2 $\Delta\gamma$	3 $\Delta\gamma$	97	145
Braces – L120x90x12	Tension	ΔL_y=4mm	7 ΔL_y	9 ΔL_y	35	46
	Compression	-	-	-	-	13

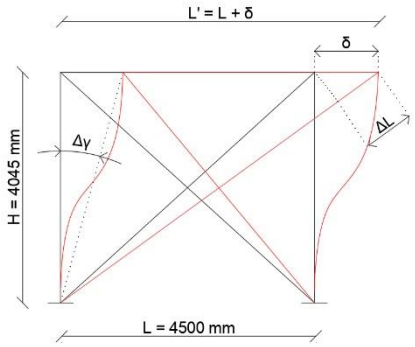

Fig. 16 Calculation scheme for rigid beam displacement

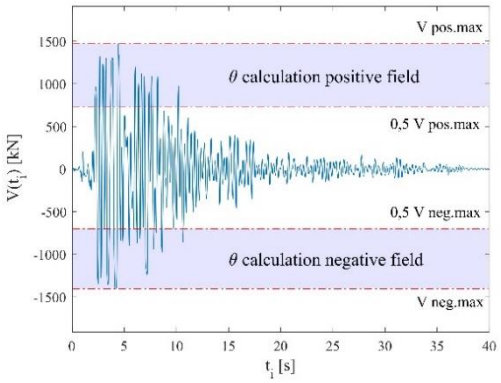

Fig. 17 Base shear recorded during the application of a ground motion

the bracings in compression, the Eurocode does not explicitly define a limit for the elastic or plastic deformation, simply defining a value for the buckling force. However, having taken into account the post-critic behavior of these elements through the insertion of the initial local bow imperfection, see Fig. 14, it was assumed that the Near Collapse limit state is reached when the element shows a reduction of the resisting force equal to the 20% of the maximum force. For each limit state, as resumed in Table 5, are evaluated the corresponding maxium deformations (chord rotation $\Delta\gamma$ for the columns and ΔL for the braces, see Fig. 16) in the hypothesis of rigid beam. The table reports also the rigid displacement δ of the beam corresponding to each limit state.

The collapse for global buckling of the structure ischecked adopting through the sensitivity coefficient to the II order effects as defined by the Eurocode 8 (EN 1998-1-2013). and evaluated as follows

$$\theta(t_i) = \frac{P \cdot \delta(t_i)}{V(t_i) \cdot H} < 0{,}3 \tag{5}$$

where P is the total vertical load acting on the building, $\delta(t_i)$ and $V(t_i)$ are respectively the horizontal displacement of the beams and the global shear at the base of the columns evaluated at the instant t_i, H is the height of the columns.

Considering that during the cyclic action the shear $V(t_i)$ can assume very low values (e.g., due to the passage of the structure to the resting position), the coefficient $\theta(t_i)$ is evaluated only when $V(t_i)$ is "sufficiently" high, meaning in this particular case $V(t_i)$>0,5V_{max}, where Vmax is the maximum base shear recorded during the application of each ground motion, see Fig. 17.

3.3 Seismic behaviour in the as-it-is configuration

The structural behavior of the case study structure under the seismic action is represented in terms of IDA curves of maximum displacements, Fig. 18, residual displacements, Fig. 19, sensitivity to second order effects, Fig. 20, and energy dissipation, Fig. 21.

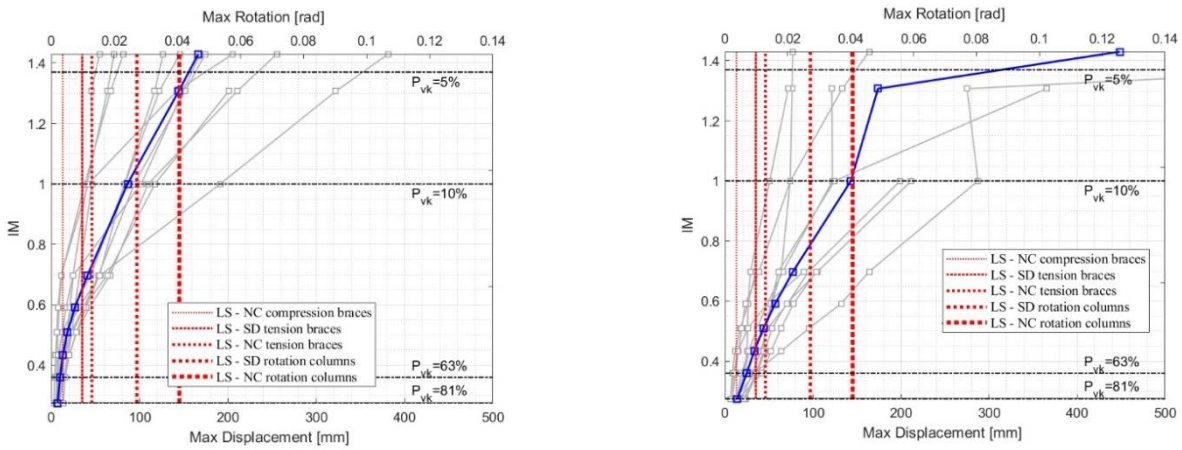

(a) (b)

Fig. 18 IDA curves of maximum displacements for the case of silos (a) 50% and (b) 75% full. The blue line represents the mean IDA curve.

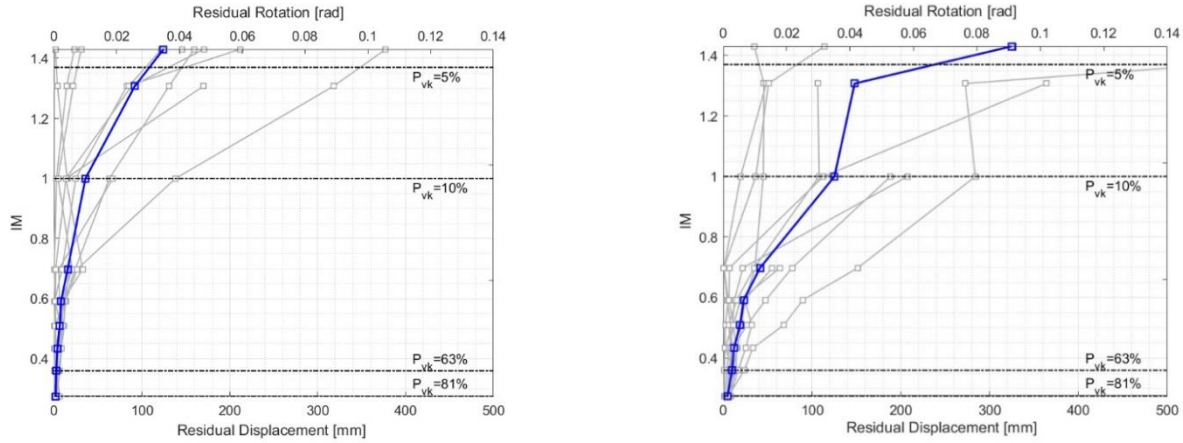

(a) (b)

Fig. 19 IDA curves of residual displacements for the case of silos (a) 50% and (b) 75% full. The blue line represents the mean IDA curve

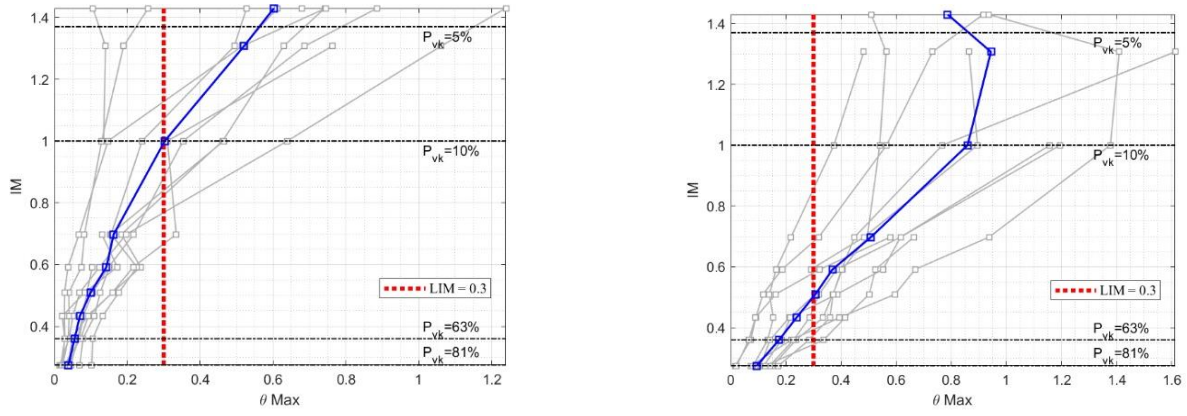

(a) (b)

Fig. 20 IDA curves of theta factor, as defined in equation (5) for the case of silos (a) 50% and (b) 75% full. The blue line represents the mean IDA curve

Fig. 18 shows that the bracings make the structure particularly sensitive to the seismic action, reaching the Near Collapse Limit State, first in compression and then in tension, even for very limited earthquake intensities. This aspect is clearly more relevant for the case of silos filled up the 75% of the maximum capacity, being characterized by a higher seismic mass. The Limit States related to the maximum plastic rotation of beams and columns are

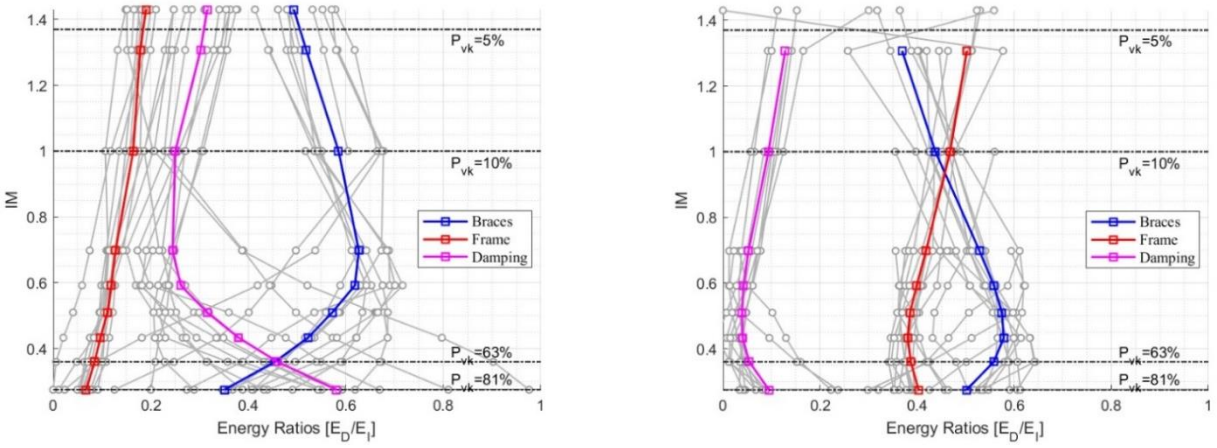

(a) (b)

Fig. 21 IDA curves of the seismic energy dissipated by the hysteretic behavior of the bracings and of the beams and columns for the case of silos (a) 50% and (b) 75% full

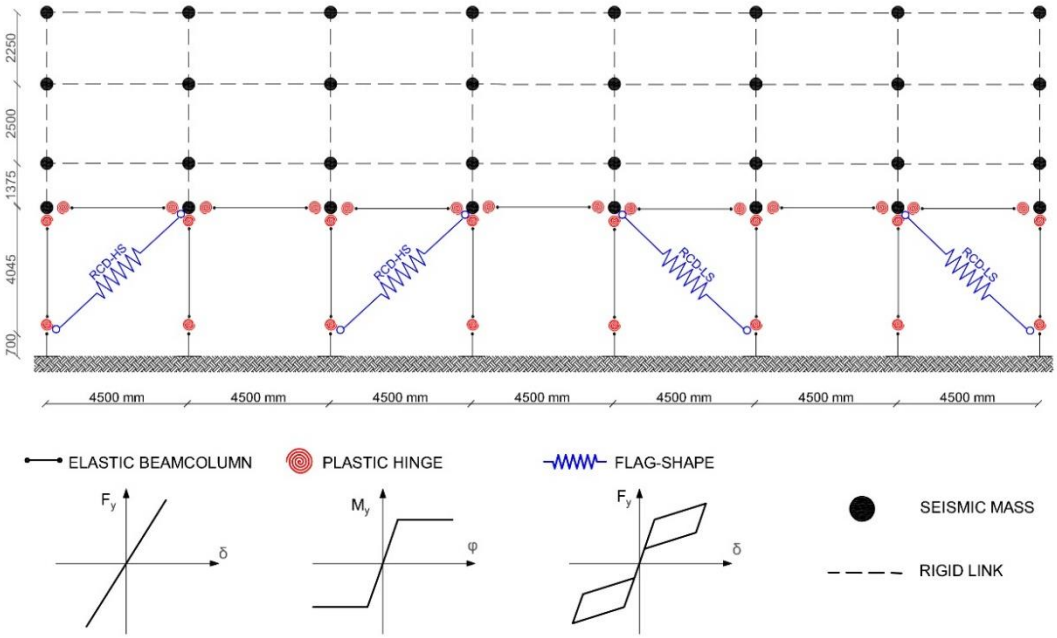

Fig. 22 Global view of the numerical model with the localization of the RCDs substituting the existing bracings

reached only for higher levels of the seismic action. The IDA curves relative to the residual deformations, in the present research evaluated as the mean value of displacements recorded in the last 5 seconds of the ground motions, are shown in Fig. 19. These results highlight that the structure has a good re-centering capacity only for low levels of the seismic action (up to the scale factor of 0.6), while significant residual displacements are accumulated for higher seismic intensities. The weight of the infill material strongly influences also this aspect, being the residual displacement assessed for the case of silos filled to the 75% more than double than the case filled to the 50%.

Finally, the combined effects of the relevant vertical loads and the lateral deformability of the structure after the yielding of the bracings leads to an high sensitivity to the second order effects, overcoming the limit value of 0.3 fixed by the Eurocode 8 (EN 1998-1-2013).

The analysis of the portion of the total seismic energy entering the structure dissipated by the bracings or by the beams and columns highlights even more the influence of the total mass on the seismic behavior of the structure. Indeed, for the case of silos filled to the 50% of the total capacity, the gravity structure (beams and columns) dissipates low energy, meaning that the damage due to hysteretic cycles to these elements are practically negligible, see Fig. 21. All the energy entered in the structure is dissipated by the bracings and by viscous phenomena. When the intensity of the seismic action increases, the portion of the energy dissipated by the bracings increases also and the one dissipated by viscosity decreases until the collapse for excessive deformation in compression of the bracings is reached. The Fig. 21(a) reports also the IDA curve of the energy dissipated in the hypothesis of neglecting the collapse for excessive

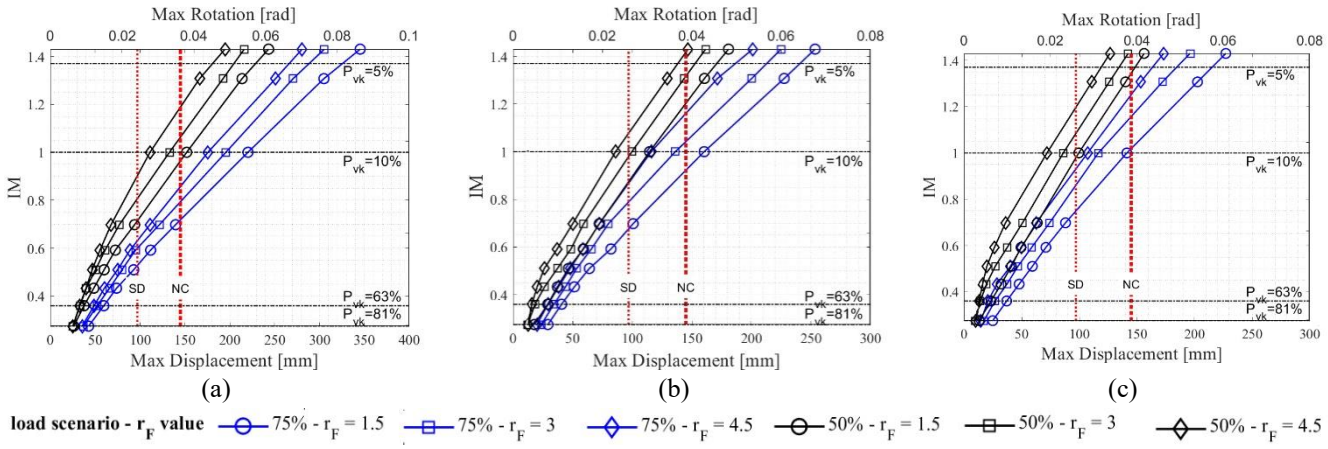

Fig. 23 IDA curves of the maximum displacement for the 9 configurations of the dissipative devices and for the 50% and 75% filling ratios: (a) r_k=2.5, (b) r_k=5, (c) r_k=7.5

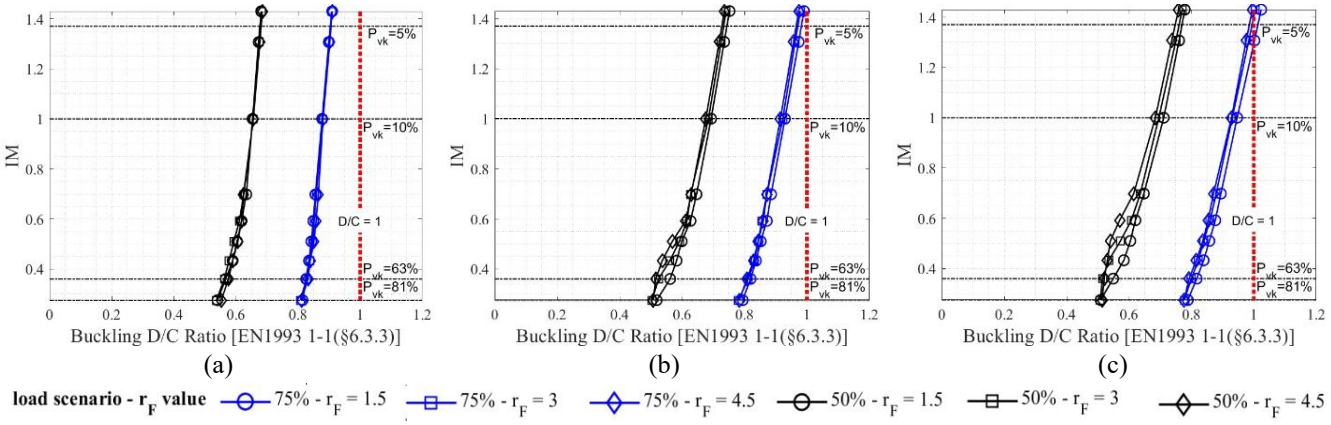

Fig. 24 IDA curves of the Demand/Capacity ratios for the buckling of the columns evaluated the 9 configurations of the dissipative devices and for the 50% and 75% filling ratios: (a) rk=2.5, (b) rk=5 and (c) rk=7.5

deformation in compression of the bracings. It shows that the maximum energy dissipation capacity is reached for a scale factor of about 0.698.

On the contrary, the case of silos filled to the 75% of the total capacity is characterized by a relevant portion of the energy dissipated by the gravity structure and by an even greater portion dissipated by the bracings, confirming the earlier collapse compared to the 50% case. Similarly to the case of silos filled to the 50%, the Fig. 21(b) reports also the IDA curve of the energy dissipated in the hypothesis of neglecting the collapse for excessive deformation in compression of the bracings. It is interesting to note that the maximum energy dissipation capacity is reached for a scale factor of about 0.433, sensibly lower than the case of silos filled to 50%, highlighting that the efficiency of the dissipation capacity of the bracings changes with the seismic intensity and the filling conditions.

4. Application of the optimization procedure to the case study

On the base of the results of the seismic vulnerability assessment on the “as-it-is” configuration of the case study building, it is evident that the bracings are not suitable to sustain even low values of the seismic action, as commonly found in structure designed only for the wind action and neglecting the seismic forces. Moreover, the structural performance is strongly influenced by the filling condition, making very difficult the choice of the new elements for the bracings especially in the case the same type of element is foreseen for all the bracings.

The structural response can be then optimized substituting the existing bracings with dissipative elements, and in particular with re-centering devices (RCDs) in order to limit the accumulation of residual displacement, and foreseeing two different groups of devices, one specifically optimized for low values of the seismic action (RCD-LS) and one for the high values (RCD-HS). The position of the devices has a low influence in the global behavior and therefore it is assumed to locate the devices in the same frame where the bracings are placed in the "as-it-is" configuration, see Fig. 22.

The research of the mechanical parameters of the RDCs that optimize the global structural response is carried in two separate steps:

- First step: research of the optimal stiffness, r_k, and yielding parameters, r_F, assuming that the two groups of devices have the same mechanical behavior.
- Second step: starting from the values of r_F and rk obtained in the first step, the optimal solution is

Table 6 Mechanical characteristics of the RCDs associated to the three multi-objective optimization scenarios for the case of silos filled to the 50%

Scenario	Weight for "$E_{DC,MAX}$ Maximization"	Weight for "Ψ Minimization"	$r_{F,LS}$	$r_{F,HS}$	α_{LS}	α_{HS}	$r_{k,LS}$	$r_{k,HS}$	$E_{DC,MAX}$	$E_{DC,MIN}$	Ψ
1	1.00	0.00	2.50	4.50	0.15	0.15	3.00	2.00	77%	59%	18%
2	0.5	0.5	1.50	6.50	0.20	0.10	3.00	2.00	75%	68%	7%
3	0.00	1.00	1.50	6.50	0.20	0.10	3.00	2.00	75%	68%	7%

searched differentiating the mechanical parameters of the two groups of RCDs, assuming a constant value for the β factor of 0.9. The second step of optimization is firstly applied to the case of silos filled to the 50% of the total capacity and then the efficacy of the optimized solution found is assessed also for the case of silos filled to the 75%.

4.1 First step of the optimization procedure

The results of the optimization carried out on the benchmark showed that a high stiffness and a high opening force F_y of the devices compared to the one of the building helps in dissipating a higher portion of the seismic energy entering the structure. For these reasons, the optimization process was started looking for the value of r_k and r_F that optimizes the global behavior according to the scenarios described in Table 1 among the following values

$$r_k = \{2.5\ ,5.0\ ,7.5\} \tag{6}$$

$$r_F = \{1.5\ ,3.0\ ,4.5\} \tag{7}$$

for a total of 9 different configurations. The value of α is kept equal to 0.15 in this first step of the optimization.

Figs. 23 and 24 report the results of the IDAs in terms of maximum displacements and maximum Demand/Capacity ratios evaluated for the buckling checks of the columns as defined in Eurocode 3 (§6.3.3 – EN 1993 1-1-2011), the latter being considered the most dangerous fragile mechanism. The displacement capacity of RCDs, assessed as proposed in (Morelli *et al.* 2017a) is always higher than the displacement associated to the Near Collapse limit state of the columns. Therefore the only limit state taken into consideration are the ones associated to the columns (LD, SD, NC), see Fig. 23.

It can be observed that the increasing of both the parameters r_F and r_k induces lower maximum displacements, allowing the attainment of the collapse due to the ultimate rotation of the column (indicated as "NC" in Fig. 23) for higher values of the seismic intensities.

Concerning the fragile mechanism of buckling of the columns, it is less sensitive to the variation of r_k and r_F but it can be observed that it tends to increase, especially for the higher levels of the seismic action, when the stiffness r_k increases. Obviously, the fragile mechanism is most critical for the case of silos filled to the 75% due to the higher value of the initial compressive force acting on the columns and an increasing of the r_k value over 7.5 would mean the reaching of the collapse due to the buckling of the columns for the higher value of the seismic action. On the contrary, the case of silos filled to the 50%, there would be still

α_{LS}	α_{HS}
0.20	0.10
0.15	0.15

$r_{k,LS}$	$r_{k,HS}$
3.25	1.75
3.00	2.00

$r_{F,LS}$
1.50
2.00
2.50

$r_{F,HS}$
4.50
5.50
6.50

Fig. 25 Scheme of the variation ranges of the mechanical parameters of the RCDs. The highlighted values are an example of possible combination

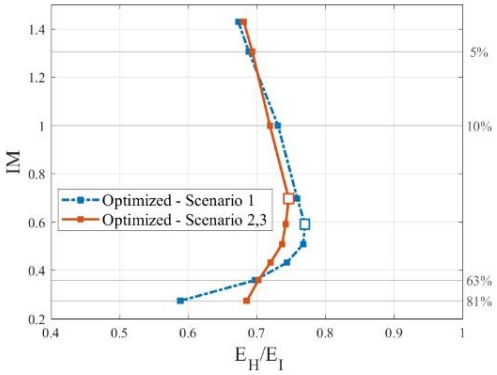

Fig. 26 IDA curves of the E_H/E_I ratio for the 50% filling ratios and for the scenario 1 and the scenarios 2 and 3

margin for a better optimization reducing the maximum displacements without overcoming the buckling resistance of the columns.

4.2 Second step of the optimization procedure

4.2.1 Filling ratio of silos equal to 50%

On the second step of the optimization procedure values of the mechanical properties are assumed different for the two groups of dissipative devices, the RCD-LS, specifically designed for low levels of the seismic action, and the RCD-HS, specifically designed for the high levels. As already anticipated in the previous sections of the paper, in order to assure a compromise between the re-centering and the dissipation capacities and to limit the parameters that need to be varied, it was assumed a constant value of β equal to 0.9. Therefore the three parameters varied in this second step are, for both the RCD-LS and the RCD-HS, the initial and post-opening stiffness, r_k (two couples of values), α (two couples of values), and the opening force r_F (nine combinations), considering a total of 36 different combinations, see Fig. 25.

Table 6 reports the results of the optimization procedure associated to the three optimization scenarios defined in Table 1.

The results of the analysis confirm that the two

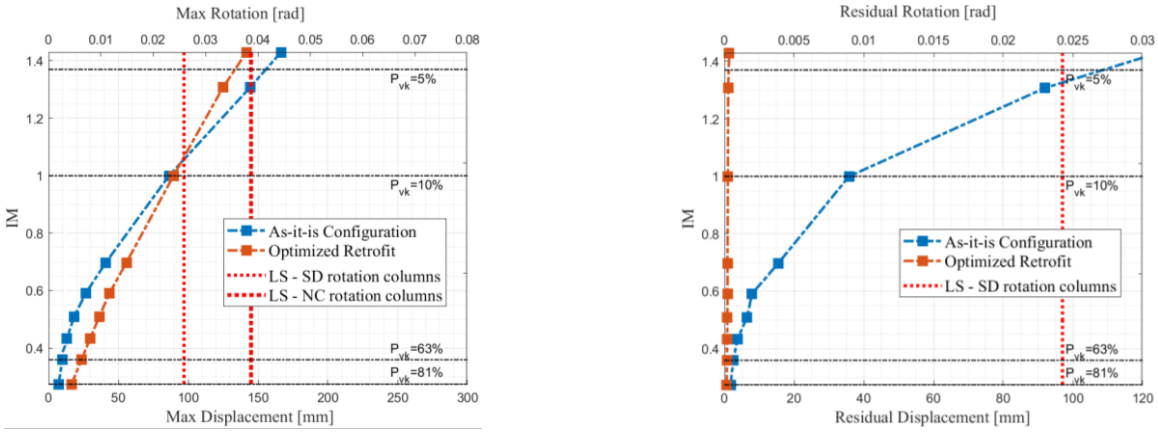

(a) (b)

Fig. 27 IDA curves in the as-it-is state and in the selected optimal retrofitted configuration for (a) the sensitivity to the II order effects (θ parameter) and (b) the Demand/Capacity ratios for the buckling of the columns

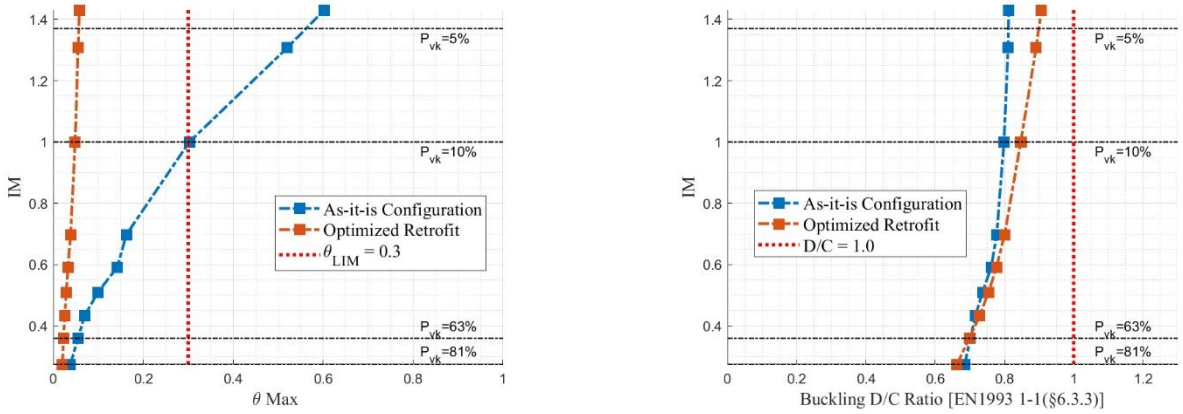

(a) (b)

Fig. 28 IDA curves in the as-it-is state and in the selected optimal retrofitted configuration for (a) the sensitivity to the II order effects (θ parameter) and b) the Demand/Capacity ratios for the buckling of the columns

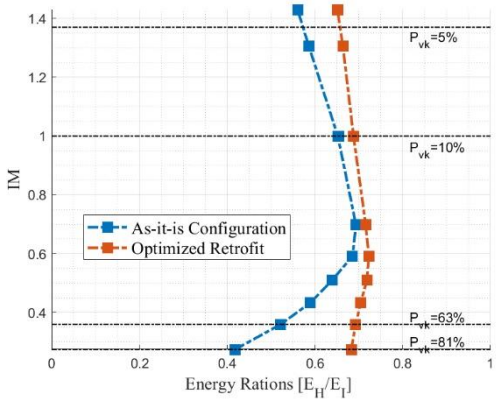

Fig. 29 IDA curves in the as-it-is state and in the selected optimal retrofitted configuration for dissipation efficiency of the RCDs

objectives of the optimization, specifically the minimization of Ψ and the maximization of E_{DC}, are antithetic and a compromise should be accepted in the multi-objective optimization process. Moreover, the mechanical properties that optimize the scenarios 2 and 3 of Table 6 are the same, indicating that an extreme minimization of the parameter Ψ, correspondent to a dissipation capacity of the system independent by the seismic intensity, is difficult to be pushed over a certain limit. The comparison of the IDA curves associated to the dissipation energy, Fig. 26, shows that both solutions are quite efficient in optimizing the dissipation of energy, being the scenario 1 characterized by higher E_H/E_I values for moderate earthquake and the scenario 2 and 3 by less variable values. The choice of the

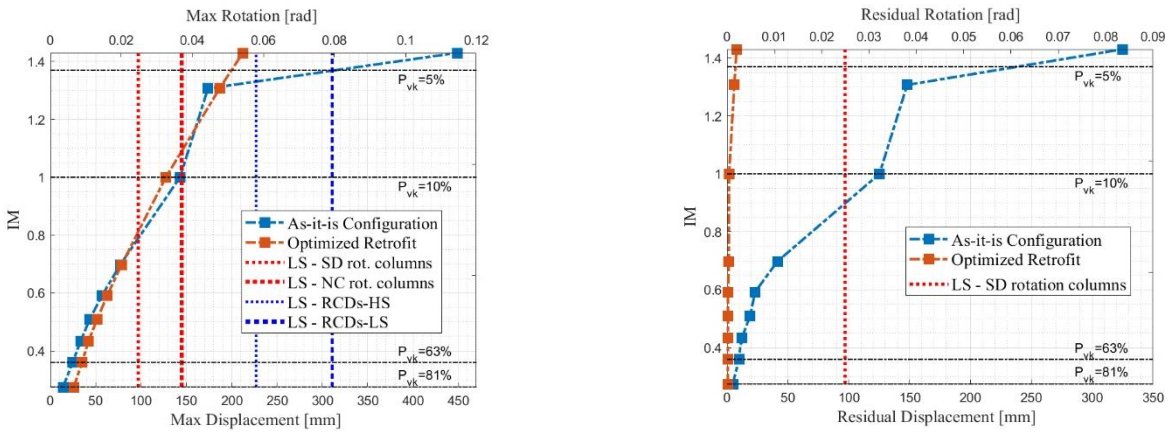

(a) (b)

Fig. 30 IDA curves in the as-it-is state with the silos filled to the 75% and in the selected optimal retrofitted configuration for the (a) maximum and (b) residual displacements

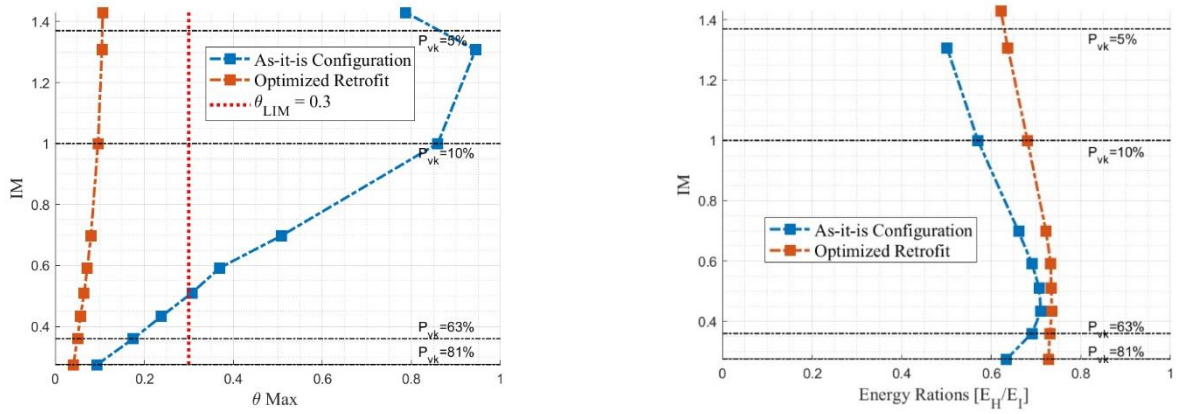

(a) (b)

Fig. 31 IDA curves in the as-it-is state with the silos filled to the 75% and in the selected optimal retrofitted configuration for (a) the sensitivity to the II order effects (θ parameter) and (b) the Demand/Capacity ratios for the buckling of the columns

desired behavior should be done on a case by case basis, depending on the objective of the retrofit.

Within this paper, it is assumed that the protection for low-to-moderate earthquake is strategic and therefore the configuration of the devices associated to scenarios 2 and 3 is chosen as the optimal one.

To better investigate the selected optimal configuration, Figs. 27, 28 and 29 reports the IDA curves associated respectively: at the maximum and residual displacements; at the sensitivity to the II order effects (θ parameter) and the Demand/Capacity ratios for the buckling of the columns as defined in Eurocode 3 (§6.3.3 – EN 1993 1-1-2011); at the dissipation efficiency.

The selected optimal solution for the retrofitting of the case study shows the capacity of reducing both the maximum and residual displacements up so that the Near Collapse limit state is not reached for any value of the seismic intensities investigated, Fig. 27(a), and the residual displacements are completely negligible, Fig. 27(b). The reduction of the displacements is reflected also in the limitation of the sensitivity to second order effects, Fig. 28(a), that are limited to values lower than 0.1 in the whole range of the seismic intensities analyzed. From the point of view of the buckling of the columns, the increased resistance of the bracings, represented by the RCDs in the retrofitted configuration, induces a general increasing of the Demand/Capacity ratio, Fig. 28(b), but the optimization process determined, however, values of such ratio always lower than 1. Finally, Fig. 29 shows the comparison between the optimized solution and the "as-it-is" configuration in terms of energy efficiency curves.

From the dissipation capacity point of view, primary objective of the optimization procedure proposed, the case study structure retrofitted with the two groups of RCDs is able to exploit a dissipation capacity practically constant over the seismic intensities and always higher than the one exhibited by the case study structure in the as-it-is configuration.

To reach this goal, the RCD-LS are characterized by a higher stiffness compared to the one of the RCD-HS, especially in the post-opening range, in which the ratio of the stiffness is equal to 3. On the contrary, in order to allow a dissipation of the seismic energy mainly for strong earthquake, the RCD-HS have a opening force 4 times

higher than the RCD-LS, whose main duty is to dissipate energy for low earthquakes. These values are certainly related to the specific characteristics of the case-study structure and cannot be generalized, but they can supply important information for the definition of the starting point of the optimization process for structures with similar characteristics.

4.1.2 Filling ratio of silos equal to 75%

The structural performance of the retrofitted case study was also assessed in the configuration with the silos filled to the 75%, characterized therefore by a higher seismic mass and higher level of compression forces on the columns.

Analogously to the silos filled to 50% case, the results of the analyses are reported in terms of IDA curves associated at the maximum and residual displacements, Fig. 30, at the sensitivity to the II order effects (θ parameter) and the Demand/Capacity ratios for the buckling of the columns, Fig. 31, and at the dissipation efficiency, Fig. 32.

The proposed retrofit solution, optimized for the case of silos filled to 50%, maintains its efficiency also in the case of percentage of filling equal to 75%. The most critical structural check is, in this case, the limitation of the maximum horizontal displacements that can induce the attainment of the plastic rotation of the columns associated to the Near Collapse Limit State. Such rotation is reached for a seismic intensity slightly higher than the one associated to the Life Safety Limit State, enhancing by little the situation with respect to the as-it-is configuration. However, from all the other points of view, the structural performance is strongly enhanced: the residual displacement is practically negligible and the buckling checks of the columns are satisfied even for the higher seismic intensities taken into account in this research, the sensitivity to second order effects is drastically reduced and the dissipation capacity is enhanced and less dependent on the seismic intensity, resulting this last aspect in a more stable and reliable dynamic behavior.

5. Conclusions

The paper presented a strategy for the optimization of the dissipative capacity of a seismic resistant system obtained placing in parallel two different groups of dissipative Re-Centering Devices (RCDs), one specifically designed to enhance the energy dissipation for the low-intensity earthquakes and the other for the high ones. Moreover, the mechanical characteristics of both groups of RCDs are selected through a multi-objective optimization process, in order to maximize the dissipation capacity and minimize the variability of such dissipation with the seismic intensity.

The application of the proposed strategy to a generic steel frame showed that, compared to the traditional case in which all the dissipative devices have the same mechanical characteristics, the differentiation in two groups allows to obtain a more efficient dissipation of the seismic energy for a wide range of the earthquake intensity values, reducing the main drawback of passive devices that are usually optimized only for a narrow range of seismic levels. Moreover, the strategy helps in maintaining the optimization also when the configuration of the building to be protected changes, for example due to the modification of the seismic mass. Similar results have been obtained also from the application of the optimization strategy to a real case study building, taking into consideration the influence of the several structural checks that needs to be done in the real practice. The proposed strategy based on the diversification of the mechanical characteristics of the RCDs, even if applied to limited case studies, showed promising perspectives and currently more studies are being carried out to analyze the influence of the mechanical behavior of the structure to be retrofitted on the optimization process.

References

Aguirre, J.J. and Almazán, J.L. (2015), "Damage potential reduction of optimally passive-controlled nonlinear structures", *Eng. Struct.*, **89**, 130-146. https://doi.org/10.1016/j.engstruct.2015.01.009.

Amouzegar, H., Riahi, H.T. and Daei, M. (2012), "Application of endurance time method in structural optimization of the dampers for seismic design", *Proceedings of the 15th World Conference on Earthquake Engineering*, Lisbon, Portugal, September.

Basu, D. and Reddy, P.R.M. (2016), "A new metallic damper for seismic resilience: analytical feasibility study", *Struct.*, **7**, 165-183. https://doi.org/10.1016/j.istruc.2016.06.011.

Belleri, A., Marini, A., Riva, P. and Nascimbene, R. (2017), "Dissipating and re-centring devices for portal-frame precast structures", *Eng. Struct.*, **150**, 736-745. https://doi.org/10.1016/j.engstruct.2017.07.072.

Braconi, A., Morelli, F. and Salvatore, W. (2012), "Development, design and experimental validation of a steel self-centering device (SSCD) for seismic protection of buildings", *Bull. Earthq. Eng.*, **10**, 1915-1941. https://doi.org/10.1007/s10518-012-9380-9.

Braga, F., Gigliotti, R. and Laguardia, R. (2019) "Intervention cost optimization of bracing systems with multiperformance criteria", *Eng. Struct.*, **182**, 185-197. https://doi.org/10.1016/j.engstruct.2018.12.034.

Christopoulos, A. and Filiatrault, C. (2006), *Principles of Passive Supplemental Damping and Seismic Isolation*, IUSS Press, Pavia, Italy

Cimellaro, G.P. (2013), *Resilience-Based Design (RBD) Modelling of Civil Infrastructure to Assess Seismic Hazards*, in *Handbook of Seismic Risk Analysis and Management of Civil Infrastructure Systems*, Woodhead Publishing Limited.

Cimellaro, G.P., Reinhorn, A.M. and Bruneau, M. (2010a), "Framework for analytical quantification of disaster resilience", *Eng. Struct.*, **32**(11), 3639-3649. https://doi.org/10.1016/j.engstruct.2010.08.008.

Cimellaro, G.P., Reinhorn, A.M. and Bruneau, M. (2010b), "Seismic resilience of a hospital system", *Struct. Infrastr. Eng.*, **6**(1-2), 127-144. https://doi.org/10.1080/15732470802663847.

CNR UNI 10011 (1988), Steel Structures – Instructions for Design, Construction, Testing and Maintenance, L. 22/04/1943 N° 633 and modifications, UNI, Milano, Italy

Dogruel, S. and Dargush, G.F. (2008), "Risk-based multi-hazard optimization of passively damped structures using evolutionary algorithms", *Proceedings of the 14th World Conference on Earthquake Engineering*, Beijing, China, October.

EN 1993-1-1 (2011), "Design of steel strucures - Part 1-1: General rules and rules for buildings", *J. Constr. Steel Res.*, **54**(2), 18-

20.
EN 1998-1 (2013), "Eurocode 8: Design of structures for earthquake resistance - Part 1: General rules, seismic asctions and rules for buildings", *J. Constr. Steel Res.*, **54**(2), 18-20.
EN 1998-3: (2005), "Eurocode 8: Design of structures for earthquake resistance – Part 3: Assessment and retrofitting of buildings, British Standards Institution.
Faggella, M., Laguardia, R., Gigliotti, R. and Morelli, F. (2016), "Performance-based nonlinear response history analysis framework for the 'PROINDUSTRY' Project", *Proceedings of the ECCOMAS Congress 2016 VII European Congress on Computational Methods in Applied Sciences and Engineering*, Crete, Greece, June.
Fateh, A., Hejazi, F., Jaafar, M.S., Karim, I.A. and Bin Adnan, A. (2016), "Design of a variable stiffness bracing system: Mathematical modeling, fabrication, and dynamic analysis", *Soil Dyn. Earthq. Eng.*, **80**, 87-101. https://doi.org/10.1016/j.soildyn.2015.10.009.
Greco, R. and Marano, G.C. (2016), "Multi-objective optimization of a dissipative connection for seismic protection of wall-frame structures", *Soil Dyn. Earthq. Eng.*, **87**, 151-163. https://doi.org/10.1016/j.soildyn.2016.01.020.
Hashemi, M.J., Al-Attraqchi, A.Y., Kalfat, R. and Al-Mahaidi, R. (2019), "Linking seismic resilience into sustainability assessment of limited-ductility RC buildings", *Eng. Struct.*, **188**(3), 121-136. https://doi.org/10.1016/j.engstruct.2019.03.021.
Hejazi, F., Toloue, I., Jaafar, M.S. and Noorzaei, J. (2013), "Optimization of earthquake energy dissipation system by genetic algorithm", *Comput. Civil Infrastr. Eng.*, **28**(10), 796-810. https://doi.org/10.1111/mice.12047.
Laflamme, S. (2018), "Passive variable friction damper for increased structural resilience to multi-hazard excitations", *Procedings of the ASME 2018 International Design Engineering Technical Conferences and Computers and Information in Engineering Conference*, Quebec City, Quebec, Canada, August.
Lee, C.H., Ryu, J., Kim, D.H. and Ju, Y.K. (2018), "Improving seismic performance of non-ductile reinforced concrete frames through the combined behavior of friction and metallic dampers", *Eng. Struct.*, **172**(12), 304–320. https://doi.org/10.1016/j.engstruct.2018.06.045.
Lin, Y.C. (2015), "Steel sliding-controlled coupled beam modules: Development and seismic behavior for a moment resisting frame", *Eng. Struct.*, **99**, 726-736. https://doi.org/10.1016/j.engstruct.2015.05.008.
Martinez-Rodrigo, M. and Romero, M.L. (2003), "An optimum retrofit strategy for moment resisting frames with nonlinear viscous dampers for seismic applications", *Eng. Struct.*, **25**(7), 913-925. https://doi.org/10.1016/S0141-0296(03)00025-7.
Mazzoni, S., McKenna, F., Scott, M.H., Fenves, G.L. and Al, E. (2007) *Open System for Earthquake Engineering Simulation (OpenSEES), OpenSEES Command Language Manual*, Pacific Earthquake Engineering Re-search (PEER) Center.
Morelli, F., Laguardia, R., Faggella, M., Piscini, A., Gigliotti, R. and Salvatore, W. (2017b), "Ground motions and scaling techniques for 3D performance based seismic assessment of an industrial steel structure", *Bull. Earthq. Eng.*, **16**(3), 1179-1208. https://doi.org/10.1007/s10518-017-0244-1.
Morelli, F., Piscini, A. and Salvatore, W. (2016), "Seismic retrofit of an industrial structure through an innovative self-centering hysteretic damper: modelling, analysis and optimization", *Proceedings of the ECCOMAS Congress 2016 VII European Congress on Computational Methods in Applied Sciences and Engineering*, Crete Island, Greece, June.
Morelli, F., Piscini, A. and Salvatore, W. (2017a), "Seismic behavior of an industrial steel structure retrofitted with self-centering hysteretic dampers", *J. Constr. Steel Res.*, **139**, https://doi.org/10.1016/j.jcsr.2017.09.025.
Morelli, F., Piscini, A. and Salvatore, W. (2019), "Development of an asymmetric re-centering dissipative device", *J. Constr. Steel Res.*, **161**, 227-243, https://doi.org/10.1016/j.jcsr.2019.07.004.
Ontiveros-pérez, S.P., Leite, R.S. and Alegre, P. (2016), "Optimal location of optimized friction dampers in civil structures for the seismic passive control", *Proceedings of the 37th Iberian Latin American Congress On Computational Methods in Engineering*, Brasilia, Brazil, November
Pekcan, G., Itani, A.M. and Linke, C. (2014), "Enhancing seismic resilience using truss girder frame systems with supplemental devices", *J. Constr. Steel Res.*, **94**, 23-32. https://doi.org/10.1016/j.jcsr.2013.10.016.
Vamvatsikos, D. (2010), "Optimal multi-objective seismic design of a highway bridge by selective use of nonlinear static and dynamic analyses", *Proceedings of the 9th International Conference on Structural Safety and Reliability (ICOSSAR)*, Osaka, Japan
Wu, B., Ou, J. and Soong, T.T. (1997), "Optimal placement of energy dissipation devices for three-dimensional structures", *Eng. Struct.*, **19**(2), 113-125. https://doi.org/10.1016/S0141-0296(96)00034-X.

CC